

FUDMA Journal of Sciences (FJS) ISSN online: 2616-1370 ISSN print: 2645 - 2944

Vol. 9 No. 11, November, 2025, pp 157 – 166 DOI: https://doi.org/10.33003/fjs-2025-0911-3992



GREY RELATIONAL ANALYSIS (GRA) OF TRIBOLOGICAL AND THERMAL PROPERTIES OF COW HOOF – REINFORCED BRAKE PADS

*Victor Ndaraba Haruna and Sulaiman Ibrahim

Mechanical Engineering Department, Federal Polytechnic, Bida, Niger State.

*Corresponding Author's Email: skishk2009@gmail.com

ABSTRACT

This study investigates and optimizes the tribological and thermal performance of cow hoof (CH)–reinforced brake pads using Grey Relational Analysis (GRA). The brake pad was produced using CH as the reinforcement material alongside with other additives which are binder (epoxy and hardener), graphite, calcium carbonate and aluminum oxide. These additives were in the proportion of 25 %, 25 %, 10 %, 30 % and 10 % by weight respectively. The produced brake pads were subjected to wear rate and coefficient of friction (COF) tests. GRA was used to obtain values of the moulding parameters that yielded optimum performance. The values of the wear rate and COF of the optimized sample are 0.197 mg/m and 0.781 respectively. Further characterisation revealed a thermal conductivity of 0.0248 W/mK. Thermo-gravimetric analysis (TGA) reveals that while asbestos-based brake pad has a better thermal stability than the CH - reinforced brake pad, the CH -reinforced brake pad has its maximum decomposition at elevated temperature range of 300 °C – 400 °C, which falls within the average brake temperature range. The experimental results of the produced brake pad compared well with the commercial and other existing experimental brake pads, demonstrating CH as a novel agro-waste material for sustainable, asbestos-free brake pad production.

Keywords: Brake pad, Coefficient of friction, Cow hoof, Moulding pressure, Thermo-gravimetric analysis, Wear rate

INTRODUCTION

The importance of brake pad in automotive vehicles that are using disc brakes cannot be overemphasized. The essence of brakes in a vehicle is to slow down or bring the vehicle to rest when desired (Ilie and Cristescu, 2023; Cracium et al., 2016). Braking is achieved by converting the dynamic energy of the vehicle to heat energy by means of friction and dissipating the heat to the surrounding atmosphere (Maleque et al., 2012). Brake pads are composed of steel backing plates with friction material bound to the surface contacting the disc (Yawas et al., 2016). Most vehicles in the present time use disc brakes due to their better heat dissipation, hence resulting to less brake fade when compared to drum brakes (Ampadu et al., 2023; Bono and Dekyrgers, 2010). Brakes are not only to bring the moving vehicle to rest but to do that at the shortest possible distance. This can only be accomplished through appropriate formulations of selected materials in the right proportions. However, not all brake pad materials are suitable for use in automobiles due to environmental pollution and other health hazards associated with them. Thus, the need to develop new materials that are considerably safe and at the same time having the required properties becomes necessary to overcome the above-mentioned challenges (Ayogwu et al.,

Brake pads are classified into semi-metallic, non-asbestos organic (NAO), low-metallic NAO and ceramic depending on their compositions. Materials for producing brake pads are categorized into binders, fillers, modifiers and reinforcements (Dagwa and Ibhadode, 2006; Maleque *et al.*, 2012; Umamaheswara, 2015). Generally, brake pads consist of asbestos fibres embedded in polymeric matrix along with several other ingredients. Despite the good mechanical and tribological properties of asbestos based brake pads, the use of asbestos in brake pad production has been avoided due to its carcinogenic nature (Aigbodion *et al.*, 2010). This draws the attention of researchers towards using either industrial or agricultural wastes which are environmentally friendly and

non-toxic materials to replace asbestos in a control composition with other ingredients in the production of brake pads (Ayogwu *et al.*, 2020). Several studies on the use of ecofriendly materials like palm kernel shell, coconut shell, banana peels, sugarcane bagasse, seashell, maize husk, periwinkle shell, and saw dust have been carried out. The use of these wastes provided economic benefits and may also result to foreign exchange earnings and environmental sanitation (Yuvaraj and Jeyanthi, 2015).

Cow hoof (CH), a largely underutilized biowaste from the meat industry, offers a distinctive reinforcement candidate. Unlike plant-based fibres, CH is keratin-rich, tough, and biodegradable, with the potential to enhance wear resistance and thermal stability in friction composites (Sellami and Elleuch, 2024). Despite its abundance and sustainability benefits, CH has not been adequately investigated as a tribomaterial, leaving a clear research gap in sustainable brake pad development (Sellami and Elleuch, 2024).

Several eco-friendly brake pad materials now demonstrate competitive performance; however, ongoing research continues to optimize their properties to fully match or surpass those of traditional asbestos-based pads. Majority of these studies used trial and error method which is time consuming to determine their properties (Irawan et al., 2022; Naidu et al., 2024; Joshi et al., 2023). Few studies have applied structured design of experiments to optimize the manufacturing parameters of asbestos-free brake pads. This study introduces CH as a sustainable reinforcement material and, more importantly, applies Taguchi design of experiments in combination with Grey Relational Analysis (GRA) to identify optimal processing conditions. The use of GRA provides an innovative multi-criteria decision tool that ensures the agricultural waste-based brake pads achieve balanced mechanical and tribological performance, thereby strengthening their potential for industrial adoption.

MATERIALS AND METHODS

CH was used as the reinforcement material while epoxy and hardener used as binder. The binder is to maintain the pad's structural integrity under mechanical and thermal stresses thereby holding the components of the brake pad together and preventing its constituents from crumbling apart. Other materials used are calcium carbonate (CaCO₃), graphite rods, aluminium oxide (Al₂O₃), sodium hydroxide (NaOH) and distilled water. The CaCO₃ was used as filler material for the purpose of improving manufacturability of the brake pad, graphite rods were ground to powder and used as the friction modifier, Al₂O₃ was used as the abrasive to increase the coefficient of coefficient (COF) and to remove iron oxides from the counter friction material as well as other undesirable surface films formed during braking (Umamaheswara, 2015), NaOH solution having 10% concentration was used to treat the reinforcement and the distilled water was used to wash away the presence of the NaOH in the treated reinforcements before drying.

Preparation of the Reinforcement Material

The CH collected was soaked in a solution of water and detergent for 30 minutes for easy removal of dirt and other contaminants and thereafter washed and sun dried to constant weight after which it was ground using milling machine. The ground CH was treated with 10 % sodium hydroxide (NaOH) solution and dried to constant weight in a similar method adopted by Abutu *et al.* (2018) and Adah *et al.* (2024). The estimated drying time was 12 hours. This treated CH powder was then sieved using sieve mesh of 150 µm. The essence of the chemical treatment of the reinforcements was to modify their surfaces and render them more hydrophobic and more compatible with the resin matrix thus improving the ultimate tensile strength of the developed brake pads (Pujari *et al.*, 2014).

Brake Material Formulation and Design of Experiment

Formulation of the brake pad sample was done using rule of mixture theorem as adopted by Abutu *et al.* (2018) and Adah *et al.* (2024). To use this theorem, the density and volume fraction of each constituent of the brake pad were first determined using a specified weight percent. This specified weight percent used was the composition that gave results that are in close agreement with results from similar research. The composition of the resin, CH, CaCO₃, graphite and Al₂O₃ used was 25%, 25%, 30%, 10% and 10% by weight respectively. The volume fraction of the CH reinforced composite was calculated using equation 1 according to Abutu *et al.* (2018).

$$V_i = \frac{w_i}{p_i} \div \sum_{j} \frac{w_j}{p_j} \tag{1}$$

Where, V_i , W_i , W_j , P_i , P_j are volume fraction of individual constituent, weight percent of the individual constituent, weight percent of the total constituents, density of the individual constituent and density of the total constituents respectively.

The theoretical density of the developed composite was calculated using equation 2.

$$\rho_{CH} = \rho_h V_h + \rho_g V_g + \rho_f V_f + \rho_a V_a + \rho_m V_m \tag{2}$$

Where ρ_{CH} , ρ_h , ρ_g , ρ_f , ρ_a and ρ_m are the densities of CH, graphite, calcium carbonate, aluminium oxide and matrix (resin) respectively. The densities of the constituents were determined using Archimedes principle. And the volume fractions of the graphite, calcium carbonate, aluminium oxide and matrix (resin) are V_h , V_g , V_f , V_a and V_m respectively.

The experimental design was built in accordance with standard Taguchi's L_{27} (3)⁴using Minitab 17 statistical software. Tables 1 and 2 showed the factor levels of the manufacturing parameters and experimental matrix with control factors respectively.

Table 1: Factor Levels for Moulding Parameters

S/N	Factors		Levels				
		1	2	3			
1	MP (MPa)	11	13	15			
2	MT (°C)	80	90	100			
3	Mt (min)	7	9	11			
4	PCt (hour)	1	1.5	2			

Where, MP, MT, Mt and PCT are moulding pressure, moulding temperature, moulding time and post curing time respectively.

Table 2: Experimental Matrix for Taguchi Design Layout

Run	MP (MPa)	MT (°C)	Mt (min)	PCt (hour)
1	11	80	7	1
2	11	80	7	1
3	11	80	7	1
4	11	90	9	1.5
5	11	90	9	1.5
6	11	90	9	1.5
7	11	100	11	2
8	11	100	11	2
9	11	100	11	2
10	13	80	9	2
11	13	80	9	2
12	13	80	9	2
13	13	90	11	1
14	13	90	11	1
15	13	90	11	1
16	13	100	7	1.5
17	13	100	7	1.5
18	13	100	7	1.5
19	15	80	11	1.5
_20	15	80	11	1.5

Run	MP (MPa)	MT (°C)	Mt (min)	PCt (hour)
21	15	80	11	1.5
22	15	90	7	2
23	15	90	7	2
24	15	90	7	2
25	15	100	9	1
26	15	100	9	1
27	15	100	9	1

Casting of the Developed Composite Samples

Powders of CH, calcium carbonate, graphite, and aluminium oxide were mixed in specified weight ratios, then combined with epoxy resin and hardener (2:1 ratio) to form a homogeneous mixture. The blend was compression-moulded in a foil-lined metallic mould and subsequently post-cured in an oven at different temperatures and times, following methods similar to Dagwa and Ibhadode (2008) and Deepika et al. (2013).

Wear Tests

The wear rate test was performed in two stages. In the first stage, samples prepared according to the Taguchi design were tested following ASTM D4966-98 (Abutu et al., 2018) using Martindale Abrasion Testing Machine (SATRA TECHNOLOGY, S/N 11884, STM:105, 230-1-50) operating at 50 rev/min. Each 38 mm × 5 mm specimen was abraded against a 135 mm stainless-steel disc coated with detachable fabric for 1000 cycles (1200 s) under a pressure of 1.26 MPa. After testing, the specimens and abraded particles were collected, and wear parameters (including wear rate, weight loss, sliding distance, wear index, wear cycle, and abrasion resistance) were determined using equations 3 to 7 (Sunday et al., 2021).

$$Wear \ rate = \frac{\Delta w}{m} \ (mg/m) \tag{3}$$

$$sliding\ distance = 2\pi Ndt(m)$$
 (4)

$$Wear index = \frac{(A-B)\times 100}{c} \tag{5}$$

$$Wear \ cycle = \frac{D}{T} \tag{6}$$

Abrasion Resistance =
$$\frac{(X-Y)\times 100}{(\%)}$$
 (%)

Wear rate =
$$\frac{\Delta w}{s}$$
 (mg/m) (3)
sliding distance = $2\pi N dt$ (m) (4)
Wear index = $\frac{(A-B)\times 100}{C}$ (5)
Wear cycle = $\frac{D}{T}$ (6)
Abrasion Resistance = $\frac{(X-Y)\times 100}{X}$ (%) (7)

Where, ΔW is the Weight loss (A-B) (mg), N is the Machine Speed in rev/min, d is the disc diameter in m, t is the time of each sample to undergo abrasion in s, A is the weight of sample before abrasion, B is the weight of sample after abrasion, C is the number of test cycle, D is the number of required cycle, T is the thickness of sample, X is the breaking force of sample before abrasion, and Y is the breaking force of sample after abrasion. The second part of the wear test was carried out on the optimised samples using the same equipment.

Coefficient of Friction (COF) Test

The inclined plane test was conducted following the Standard Organization of Nigeria (SON) procedure, as adapted from Ademoh and Olabisi (2015). Both the plane and specimens were cleaned before testing, and the plane was fixed at an angle of 15°. Each specimen was mounted on a mild steel slider using adhesive, and the combined weight of the specimen and slider was measured (Figure 1). A 5 N hanger was attached via a cord, and additional load was gradually applied until the specimen began to slide up the plane. The corresponding load was recorded, and the procedure repeated for all samples. The coefficient of static friction for each specimen was then calculated using equations 8 and 9.

$$W = mg$$

$$\mu = \frac{F - WSine}{WCose}$$
(8)

Where, W, M, g, µ, F and Θ are weight of the specimen together with the slider in N, mass of the specimen together with the slider in kg, acceleration due to gravity in m/s², COF, applied load in N and angle of inclination in degrees respectively.

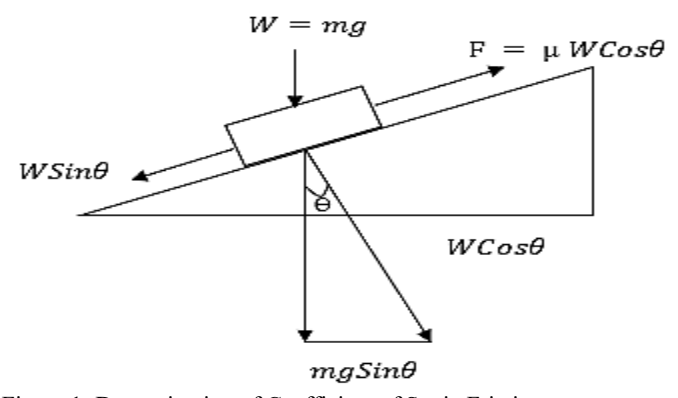


Figure 1: Determination of Coefficient of Static Friction

Taguchi and GRA Analysis

Signal-to-noise (S/N) ratio and variance analyses were performed on the characterization results to evaluate the significance of manufacturing parameters on the responses and achieve optimization. Design Expert 12 software was used to develop empirical regression models. Two quality characteristics proposed by Abutu *et al.* (2018) were applied. Smaller – the – better: $\frac{s}{N} = -10 \log \frac{1}{n} (\sum_{i=1}^{n} x^2)$ (10)

Larger – the – better:
$$\frac{s}{N} = -10 \log \frac{1}{n} \left(\sum_{i=1}^{n} \frac{1}{x^2} \right)$$
 (11)
Where n and x are number of experimental samples and

responses of given factor level combination.

The empirical model equations can be used to study changes in the values of responses (dependent variables) as one of the independent variables (MP, MT, Mt and PCT) is varied while others are kept constant. A validation test for all the responses was carried out using the optimal values of the manufacturing parameters obtained from the GRA in order to know extent of reliability of the developed empirical model equations. The result of validation test was used to calculate percentage error between the experimental and calculated values of the

GRA was conducted on the response values with the aim of compressing the multi-response parameters into a single response. The first stage of GRA involved the experimental design using Taguchi technique, followed by signal-to-noise (S/N) ratio calculation of responses using smaller-the better (wear rate) and larger-the better (friction coefficient) quality characteristics shown in equations 10 and 11 respectively. S/N ratio calculation was followed by calculation of grey relational generating (GRG) using equation 12 (smaller-thebetter attributes) and 13 (larger-the-better attributes). GRG was conducted to normalize the S/N ratio values in the range between 0 and 1 (Abutu et al., 2018).

$$Smaller - the - better attributes = \frac{x_{ij} - x_{ij}}{\overline{x_j} - \underline{x_j}}$$
 (12)

Smaller – the – better attributes =
$$\frac{x_{ij} - x_{ij}}{\overline{x_i} - x_j}$$
 (12)
Larger – the – better attributes = $\frac{x_{ij} - x_{ij}}{\overline{x_i} - x_j}$ (13)

Where, x_{ij} is the individual response value and $\overline{x_i} = \max \{x_{ij}, x_{ij}\}$ i=1, 2...m} and $x_i = min \{x_{ij}, i=1, 2, ..., m\}.$

The GRG procedure is followed by the calculation of grey relational coefficient (GRC) using equation 14.

$$\textit{GRC} = \frac{\Delta_{\text{min}} + \lambda \Delta_{\text{max}}}{\Delta_{\mathit{ij}} + \lambda \Delta_{\text{max}}} \, (i\text{=}\,1,2\dots m \text{ and } j\text{=}\,1,2\dots n)$$

Where $\Delta_{ij} = x_{0j} - x_{ij}$ while $\Delta_{min} = \min(0)$ and $\Delta_{max} =$

 λ is the distinguishing coefficient, $\beta \in [0, 1]$.

Distinguishing coefficient ($\tilde{\lambda}$) is used to expand or compress the range of the GRC and 0.5 is the accepted value (Abutu et al., 2019).

Thermal Conductivity Test

Thermal conductivity (k) was measured using Searle's apparatus following the method of Ademoh and Olabisi (2015). Rectangular specimens were used, with one end inserted into a steam chamber and the other cooled by water flowing through a coiled copper tube. Temperatures of the specimen (T1, T2) and water flow (T3, T4) were monitored

until steady state was reached. The entire setup was insulated to minimize heat loss, and the recorded values were used to calculate thermal conductivity. The thermal conductivity is calculated using equation 15.

$$k = \frac{VIA}{\Delta T} \tag{15}$$

Where, k is the thermal conductivity of the specimen in W/mK, V is the Voltage in the circuit in volts, I is the Current flowing in the circuit in amperes, A is the Area of the specimen in m^2 , Δ is the Temperature difference $(T_1 - T_2)$ in Kelvin, T is the Thickness of the specimen in m.

Thermo-Gravimetric Analysis (TGA)

Thermo-gravimetric analysis (TGA) was conducted to assess the thermal stability of the samples using a Thermogravimetric Analyzer, which records mass loss as a function of temperature (Ruzaidi et al., 2011). Approximately 10-14 mg of each sample was placed in a 6.4 mm × 3.2 mm open pan and heated from 30 °C to 950 °C at 10 °C/min under a continuous nitrogen flow of 60 mL/min. Prior to each run, the furnace was purged with nitrogen for 30 minutes to establish an inert environment and prevent oxidative decomposition. Thermogravimetric (TG) and differential thermal analysis (DTA) curves were generated using Universal Analysis 2000 software (TA Instruments).

RESULTS AND DISCUSSION **Brake Pad Formulation using Rule of Mixture**

The formulation gave a predicted density of the developed brake pad to be 1.203 g/cm³ when produced. This predicted value obtained from the result is in close agreement with the recommended values of commercial asbestos brake pad that has density values ranging from 1.01 - 2.06 g/cm³ as reported by Ikpambese et al. (2014); Abutu et al. (2018) and Abutu et al. (2019). The mass of the developed brake pad is targeted at the mass of the commercial asbestos brake pad (176 g) as reported by Ikpambese et al. (2014).

Brake Pad Samples

The brake pad samples produced following the Taguchi experimental Design Matrix (Table 2) are shown in Figure 2.



Figure 2: CH -Reinforced Brake Pad Samples

Characterization of the Developed Brake Pad

The results obtained and the signal-noise ratios calculated for wear and COF tests are shown in Table 3.

Table 3: Experimental Results for the Developed Brake Pad

	•		Mt	DOT (1	Wear rate	COF	Wear rate	COE (IB)
Run	MP (MPa)	MT (°C)	(min)	PCT (hour)	(mg/m)	(μ)	(dB)	COF (dB)
1	11	80	7	1	0.23576	0.775	12.5508	-2.2091
2	11	80	7	1	0.39292	0.739	8.1138	-2.6295
3	11	80	7	1	0.31434	0.692	10.0520	-3.1987
4	11	90	9	1.5	0.13752	0.769	17.2325	-2.2844
5	11	90	9	1.5	0.35363	0.877	9.0290	-1.1425
6	11	90	9	1.5	0.27505	0.742	11.2119	-2.5867
7	11	100	11	2	0.13752	0.688	17.2325	-3.2450
8	11	100	11	2	2.06285	0.738	-6.2894	-2.6420
9	11	100	11	2	0.11788	0.795	18.5714	-1.9922
10	13	80	9	2	0.11788	0.782	18.5714	-2.1333
11	13	80	9	2	0.05894	0.868	24.5920	-1.2310
12	13	80	9	2	0.35363	0.790	9.0290	-2.0500
13	13	90	11	1	0.09823	0.864	20.1550	-1.2726
14	13	90	11	1	0.09823	0.850	20.1550	-1.4136
15	13	90	11	1	0.25540	0.670	11.8556	-3.4810
16	13	100	7	1.5	0.29469	0.751	10.6125	-2.4820
17	13	100	7	1.5	0.11788	0.631	18.5714	-4.0021
18	13	100	7	1.5	0.11788	0.831	18.5714	-1.6029
19	15	80	11	1.5	0.09823	0.810	20.1550	-1.8251
20	15	80	11	1.5	0.45186	0.713	6.8999	-2.9380
21	15	80	11	1.5	0.13752	0.759	17.2325	-2.3905
22	15	90	7	2	0.47151	0.875	6.5302	-1.1602
23	15	90	7	2	0.29469	0.769	10.6126	-2.2778
24	15	90	7	2	0.23576	0.813	12.5508	-1.7981
25	15	100	9	1	0.15717	0.763	16.0726	-2.3532
26	15	100	9	1	0.19646	0.796	14.1344	-1.9775
27	15	100	9	1	0.29469	0.838	10.6126	-1.5389

Wear Rate and COF Tests

Table 3 shows that the wear rate and COF of the brake pad samples change with variation in the manufacturing parameters. The wear rate of the developed samples varied from 0.05894 mg/m to 2.0628 mg/m while the COF ranges from 0.631 to 0.877. The improved COF at higher moulding pressures is attributed to better bonding between CH fibres and resin matrix. These COF values are within the class H (> 0.55) type of brake pads recommended by the Society of Automobile Engineers (SAE) for use in automobiles. This was also reported by Blau (2001) and Dagwa and Ibhadode (2006). Therefore, the developed brake pad is suitable for use in both light and heavy-duty automobiles.

Experimental Results Analysis

The smaller-the-better signal to noise ratio quality characteristics given in equation 12 was used to calculate the wear rate while the larger-the-better quality characteristics given in equation 13 was used to calculate the COF. The values calculated are shown in Table 3, it shows that as the values of the experimental responses increases, the S/N ratio values calculated also increases with the samples having the greatest values indicating an ideal state situation. The

empirical regression analysis of individual responses is hereby discussed. The empirical regression models for manufacturing parameters (MP, MT, Mt and PCT) were obtained from regression analysis using Design Expert 12 software to predict the properties of the developed brake pads. The regression equations for both wear rate and COF together with their corresponding regression correlation coefficients (R-sq) for the developed brake pad are shown in equations 16 and 17 respectively.

$$\begin{split} WR^{0.5} &= 9.66 - 0.993MP - 0.027MT - 0.287Mt - \\ 0.63PCT + 0.0373MP^2 + 0.000166MT^2 + 0.016Mt^2 + \\ 0.240PCT^2 & (16) \\ R - Sq &= 71.27\%, R - Sq \ (adj) = 55.35\% \\ CoF^{0.5} &= -1.38 + 0.026MP + 0.0387MT + 0.0992Mt - \\ 0.121PCT - 0.00078MP^2 - 0.000127MT^2 - \\ 0.0055Mt^2 + 0.0431PCT^2 & (17) \\ R - Sq &= 65.12\%, R - Sq \ (adj) = 56.30 \% \end{split}$$

GRA of the Experimental Results

The values calculated for grey relational generation (GRG), grey relational coefficient (GRC) and grey relational grade of the developed brake pad are shown in Table 4.

Table 4: Results of GRG, GRC and Grade (CH)

Runs	GRG		GRC	GRC		
	Coefficient of Friction	Wear rate	Coefficient of Friction	Wear rate	— Grades	
Xo	1.0000	1.0000				
1	0.6270	0.5336	0.5727	0.5174	0.5262	
2	0.4800	0.4708	0.4902	0.4858	0.4957	
3	0.2809	0.2383	0.4102	0.3963	0.5125	
4	0.6007	0.5040	0.5560	0.5020	0.4842	
5	1.0000	0.4333	1.0000	0.4687	0.5989	
6	0.4950	0.2383	0.4975	0.3963	0.5799	
7	0.2648	1.0000	0.4048	1.0000	0.6665	
8	0.4756	0.1950	0.4881	0.3831	0.5634	

Dung	GRG	GRG			Condo
Runs	Coefficient of Friction	Wear rate	Coefficient of Friction	Wear rate	— Grades
9	0.7029	0.1950	0.6272	0.3831	0.5347
10	0.6535	0.0000	0.5907	0.3333	0.4943
11	0.9691	0.5040	0.9417	0.5020	0.6864
12	0.6827	0.1437	0.6117	0.3686	0.6835
13	0.9545	0.1437	0.9166	0.3686	0.7394
14	0.9052	0.4124	0.8406	0.4597	0.7450
15	0.1822	0.4527	0.3794	0.4774	0.5147
16	0.5316	0.1950	0.5163	0.3831	0.5389
17	0.0000	0.1950	0.3333	0.3831	0.6037
18	0.8390	0.1437	0.7564	0.3686	0.6917
19	0.7613	0.5729	0.6769	0.5393	0.5278
20	0.3721	0.2383	0.4433	0.3963	0.5573
21	0.5636	0.5849	0.5340	0.5464	0.5630
22	0.9938	0.4527	0.9878	0.4774	0.6606
23	0.6030	0.3899	0.5574	0.4504	0.6051
24	0.7707	0.2759	0.6856	0.4085	0.6595
25	0.5766	0.3386	0.5415	0.4305	0.5204
26	0.7080	0.4527	0.6313	0.4774	0.6228
27	0.8614	0.7963	0.7829	0.7106	0.5958

Factor Levels of Main Effects

The factor effects for CH shown in Table 5 were obtained using Grade values from GRA as presented in Table 4.

Table 5: Resulting Factor Effects of Experimental Factors (CH)

Factor level	MP	MT	Mt	PCT	
Level 1	0.5513	0.5607	0.5882	0.5858	
Level 2	0.6331	0.6208	0.5851	0.5717	
Level 3	0.5902	0.5931	0.6013	0.6171	

Main Effect Plots for GRA

The main effect plots for GRA shown in Figure 3 specified the optimal factor levels of composite composition. These plots were obtained using the Factor Levels of Main Effects shown in Table 5.

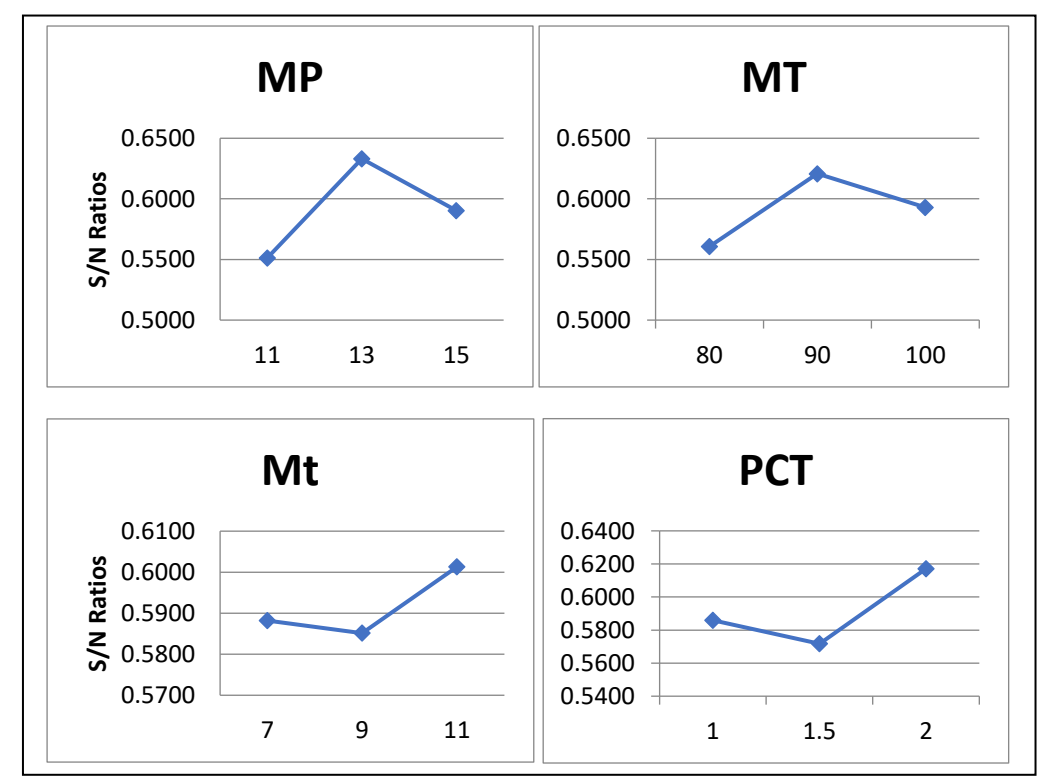


Figure 3: Main Effect Plot for GRA of the Developed Brake Pad

Figure 2 indicates that multi-response optimal factor PCT (2hours). This means that any value of the manufacturing combination are MP (13MPa), MT (90°C), Mt (11mins) and parameters used outside these optimal values may lead to poor bonding between the matrix and other constituents of the composite.

Validation Test

The validation test was carried out by comparing the experimental values (Exp) with the calculated values (Cal) and finding the percentage error (E) for individual response using equation 18. The calculated values for the responses were obtained using regression equation for individual

response presented in equations 16 and 17. The optimal values of the manufacturing parameters shown in Figure 3 were used to get the calculated values. Table 6 presents the experimental values, calculated values and the percentage error for individual response.

Percentage Error (E) = $\frac{Experimental\ Value\ (Exp) -\ Calculated\ Value\ (Cal)}{Experimental\ Value\ (Exp)} \times 100$ (18)

Table 6: Experimental and Calculated Values for the Optimised Samples

S/N	Response	Exp	Cal	E (%)
1	Wear Rate (mg/m)	0.1972	0.201	1.9
2	COF (µ)	0.7810	0.8237	5.5

It can be observed from Table 3.4 that the percentage error of COF response is a little above 5% but less than 10%. This may be attributed to the disturbance resulting from experimental environment.

The GRA results (presented in Tables 4 and 5, along with Figure 3) demonstrate how multi-response optimization compresses wear rate and COF into a single performance index. Runs with higher GRA grades correspond to brake pads with low wear rate and stable friction, indicating reliable braking under varying loads. For instance, runs 13, 14, 18 and 22, samples with high GRG values ranked top in overall performance, confirming that optimal manufacturing parameters enhance both durability and braking efficiency. The main effect plots presented in Figure 3 further established the optimal factor levels as MP = 13 MPa, MT = 900 °C, Mt

= 11 min, and PCT = 2 h. These parameters yielded pads with improved bonding between matrix and reinforcements, minimizing wear while sustaining high friction stability.

Validation tests (Table 6) confirmed the predictive accuracy of the empirical models, with percentage errors below 10% (1.9% for WR and 5.5% for COF). This level of agreement demonstrates the robustness of the regression models and the reliability of the GRA-based optimization for guiding industrial-scale production.

Thermal Conductivity of the Optimised Samples

Table 7 shows the results of the thermal conductivity test of the CH-reinforced brake pad carried out.

Table 7: Thermal Conductivity Result

Rn	Th. Conductivity (Wm ⁻¹ K ⁻¹)
СН	0.02480
CB	0.5539

Table 7 shows that the thermal conductivity of the developed brake pad is 0.02480Wm⁻¹K⁻¹. The value obtained is far below the value obtained for commercial brake pad (0.5539Wm⁻¹K⁻¹). This implies that the brake pad newly developed have better resistance to heat than the commercial asbestos-based brake pad. However, there are no readily available information on thermal conductivities of the earlier researches conducted on asbestos free brake pads for comparison except that on palm kernel shell based brake pad by Dagwa and Ibhadode (2006) with 1.46 Wm⁻¹K⁻¹, maize husk based brake pad by Ademoh and Olabisi (2015) with 0.33 Wm⁻¹K⁻¹ and

Ajibola *et al.* (2024) reporting 1.3422 Wm⁻¹K⁻¹ for sawdust respectively. Dirisu *et al.* (2024) reported even lower values of 0.007 Wm⁻¹K⁻¹ for Coconut shell and oil bean stalk. Low thermal conductivity is advantageous for braking applications, as it minimizes heat build-up at the friction interface, thereby reducing the risk of brake fade during prolonged braking.

Thermo-gravimetric Analysis of the Optimised Sample

Figures 4 and 5 show TGA/DTG graphs of CH-reinforced and commercial asbestos based brake pads respectively.

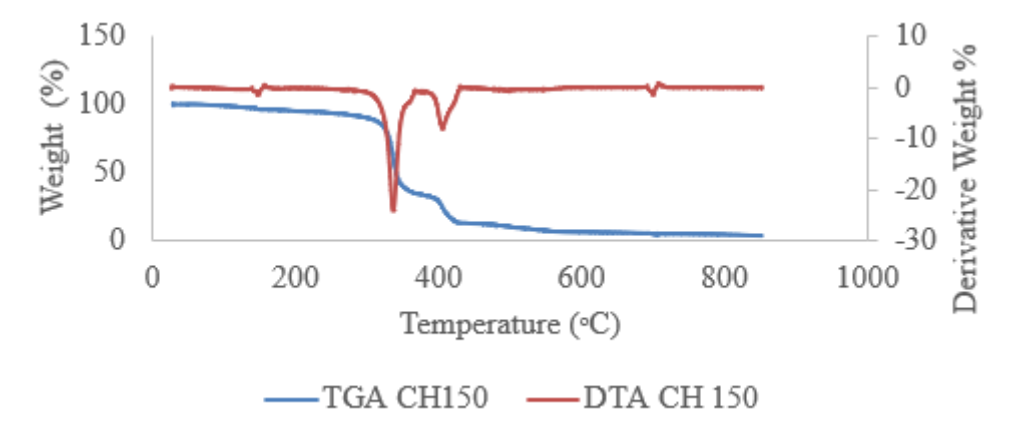


Figure 4: TGA/DTG Curves of CH-Reinforced Brake Pad

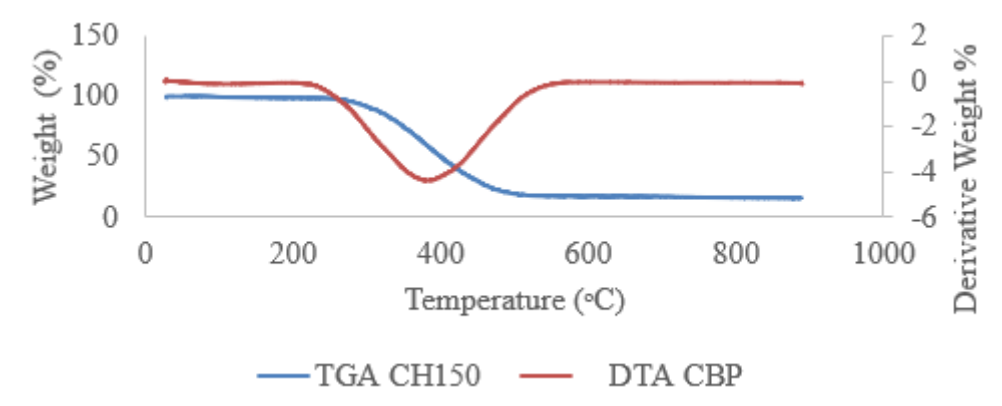


Figure 5: TGA/DTG Curves of Commercial Asbestos-Based Brake Pad (CBP)

It can be observed that Figure 4 has three zones of weight loss. The first zone which is due to loss of moisture content and volatiles is between 30 °C to 300 °C with maximum degradation at 140 °C as witnessed in DTG curve. The second zone which is as a result of further removal of moisture content is between 300 °C and 450 °C with a maximum weight loss at 450 °C. The last zone which is due to pyrolysis and oxidation is between 450 °C to 850 °C with maximum weight loss at 680 °C.

The TGA curve in Figure 5 also shows three zones of weight loss with maximum degradation at 380 °C. The three zones are between 30 °C to 280 °C, 280 °C to 500 °C and 500 °C to 900 °C. From all the TGA curves, commercial asbestos-based brake pad appeared to be the more thermally stable than CH-reinforced brake pad. However, CH-reinforced brake pad has its maximum decomposition at a higher temperature range of 300 °C to 400 °C which according to Amaren (2014) falls

within the range of average braking temperature ($300\,^{\circ}\text{C}-400\,^{\circ}\text{C}$). This suggests that the developed pad can withstand real braking conditions without premature degradation while also offering enhanced resistance to heat propagation, improving braking reliability under repeated or high-load stops.

Comparison of the Developed Brake Pads with Commercial and other Existing Experimental Brake Pads Table 8 shows the experimental values obtained for the developed brake pad compared with the values of the commercial and other existing experimental brake pads. Under SAE J661, many accepted friction materials show COFs in the range of 0.35-0.45 during the various test stages (Naidu et al., 2024; Kanagaraj et al., 2023; Akramifard and Ghasemi, 2016). Compared to those, the developed CH pads with COF 0.78 show superior friction performance under those test conditions.

Table 8: Experimental Results Compared with Commercial and other Existing Experimental Brake Pads

S/N	Author	Reinforcement material	Wear rate (mg/m)	COF (µ)
1.	Commercial	Asbestos	3.8	0.4
2.	Author	Sheanut shells	0.216	0.7103
3.	Author	СН	0.1972	0.7810
4.	Zheng et al. (2025)	Andalusite	-	0.53
5.	Ammar et al. (2024)	Date palm	1.5	0.73
6.	Dirisu et al. (2024)	Coconut shell and oil bean stalk	-	0.45
7.	Shuaibu <i>et al.</i> (2023)	Coconut shell/ash	-	0.4
8.	Naidu et al. (2022)	Hemp fibre	-	0.40
9.	Abutu et al. (2019)	Coconut shells	0.03156	0.614
10.	Abutu et al. (2019)	Seashells	0.07252	0.525
11.	Yawas et al. (2016)	Periwinkle shells	-	0.41
12.	Bala et al. (2016)	СН	2.08	0.42
13.	Ademoh and Olabisi (2015)	Maize husk	2.146	0.37-0.40
14.	Idris et al. (2015)	Banana peels	4.15-4.67	0.35-0.40
15.	Hase and Belkar (2015)	Fly ash	62-470	0.38-0.44
16.	Bashir, Saleem and Bashir (2015)	Banana peels	0.06-0.73	0.78
17.	Zhenzhen et al. (2012)	Flax fibres	0.576-0.779	0.692-0.898
18.	Aigbodion et al. (2010)	Bagasse	4.2	-
19.	Dagwa and Ibhadode (2006)	Palm kernel shell	4.4	0.43

When benchmarked against other natural reinforcements, the CH pad outperformed coconut shell pads with COF of 0.614 (Abutu *et al.*, 2019), seashells with COF of 0.525 (Abutu *et al.*, 2019), and maize husk pads with COF of 0.37–0.40 (Ademoh and Olabisi, 2015), while maintaining a significantly lower wear rate. The improvement over earlier CH composites (wear rate 2.08 mg/m; COF 0.42, Bala *et al.*, 2016) further underscores the effect of optimized processing

and formulation. Thus, the CH-reinforced pads not only meet but surpass minimum frictional requirements while offering better wear resistance than asbestos-based pads, highlighting their potential as a sustainable and high-performance replacement material.

CONCLUSION

From the results of these examinations, it was concluded that:

- The developed cow-hoof reinforced brake pad was predicted to have a density of 1.203 g/cm³ using the rule of mixture, which is within the acceptable range for friction composites.
- ii. GRA identified the optimal formulation parameters as MP (13 MPa), MT (90 °C), Mt (11 minutes), and PCT (2 hours). These conditions yielded pads with stable friction and wear properties.
- iii. TGA showed that the commercial brake pad exhibited higher overall thermal stability; however, the cow-hoof composite reached maximum decomposition within 300– 400 °C, which coincides with the average braking temperature range, confirming its practical suitability
- iv. Experimental results demonstrated that the developed brake pads achieved SAE-compliant friction properties and compared favourably with both commercial asbestos pads and other natural-fibre-based alternatives.
- v. This study establishes the novelty of valorising agricultural and slaughterhouse waste (CH) into a highperformance, eco-friendly friction composite. The findings highlight its potential as a scalable, asbestos-free alternative for automotive brake pad applications.

Further investigations are recommended to include microstructural characterization, extended durability and fade-recovery testing under dynamic braking conditions, and life-cycle assessment to strengthen the case for industrial adoption.

REFERENCES

Abutu, J., Lawal, S. A., Ndaliman, M. B., Lafia-Araga, R. A., Adedipe, O., & Choudhury, I. A. (2018). Effects of process parameters on the properties of brake pad developed from seashell as reinforcement material using grey relational analysis. Engineering Science and Technology, an International Journal, 21(4): 787-797.

Abutu, J., Lawal, S. A., Ndaliman, M. B., Lafia-Araga, R. A., Adedipe, O., & Choudhury, I. A. (2019). Production and characterization of brake pad developed from coconut shell reinforcement material using central composite design. Springer Nature Journal of Applied Sciences, 1(82), 1-15.

Adah, P. U., Nuhu, A. A., Salawu, A. A., Hassan, A. B., & Ubi, P. A. (2024). Characterization of periwinkle shell ash reinforced polymer composite for automotive application. FUDMA Journal of Sciences (FJS), 8(1), 83-92.

Ademoh, N. A., & Olabisi, A. I. . (2015). Development and evaluation of maize husks (asbestos – free) based brake pad. Industrial Engineering Letters, 5(2): 67 - 80.

Aigbodion, V. S., Akadike, U., Hassan, S. B., Asuke, F., & Agunsoye, J. O. (2010). Development of asbestos – free brake pad using bagasse. Tribiology in Industry, 32(1): 45 – 50.

Ajibola, K. A., Olaiya, K. A., & Alabi, I. O. (2024). Investigation of thermal properties and ash content of sawdust-reinforced composite brake pads. Journal of Scientific and Engineering Research, 11(7): 221-228.

Akramifard, H. R., & Ghasemi, Z. (2016). Friction and wear properties of a new semi-metallic brake pad according to SAE J 661: A case study in PARSLENT complex (Iran). International Journal of New Technology and Research (IJNTR), 2(3), 96-99.

Ammar, Z., Adly, M., Abdalkarim, S. Y. H., & Mehanny, S. (2024). Incorporating date palm fibers for sustainable friction composites in vehicle brakes. Scientific Reports, 14(1), 1-19.

Ampadu, V. M. K., Alrejjal, A., & Ksaibati, K. (2023). Performance and cost-effectiveness of air disc brakes and air drum brakes for truck semi-trailers in different road and speed conditions. Journal of Sustainable Development of Transport and Logistics, 8(1): 24-42.

Ayogwu, D. O., Sintali, I. S., & Bawa, M. A. (2020). A review on brake pad materials and methods of production. Composite Materials, 4(1): 8-14.

Bala, K. C., Okoli, M., & Abolarin, M. S. (2016). Development of automobile brake lining using pulverized cow hooves. Leonardo Journal of Sciences, 2(28): 95-108.

Bashir, M., Saleem, S. S., & Bashir, O. (2015). Friction and Wear Behaviour of Disc Brake Pad Material using Banana Peel Powder. International Journal of Research in Engineering and Technology, 4(2): 650 – 659.

Blau, P. J. (2001). Compositions, functions and testing of friction brake materials and their additives: a report by oak ridge national laboratory for U.S dept. of energy. USA: U.S Dept. of Energy.

Bono, D. S., & Dekyrger, W. J. (2010). Auto technology, theory and services. New York: DELMAR Publishers.

Cracium, A. L., Pinca-Bretotean, C., Birtok-Baneasa, C., & Josan, A. (2016). Composites materials for friction and braking application. Innovative Ideas in Science, 200(1), 1-5.

Dagwa, I. M., & Ibhadode, A. O. A. (2006). Determination of optimum manufacturing conditions for asbestos-free brake pad using Taguchi method. Nigerian Journal of Engineering Research and Development, 5(4): 1-8.

Dagwa, I. M., & Ibhadode, A. O. A. (2008). Development of asbestos – free friction lining material from palm kernel shell. Journal of the Brazilian Society of Mechanical Scientists and Engineers, 1(2): 166 – 173.

Deepika, K., Reddy, C. B., & Reddy, D. R. (2013). Fabrication and preformance evaluation of composite material for wear resistance application. International Journal of Engineering Science and Innovative Technology (IJESIT), 2(6): 66 – 71.

Dirisu, J. O., Okokpujie, I. P., Apiafi, P. B., Oyedepo, S. O., Tartibu, L. K., Omotosho, O. A., Ogunkolati, E. O., Oyeyemi, E. O., & Uwaishe, J. O. (2024). Development of eco-friendly brake pads using industrial and agro-waste materials. Journal of Engineering and Applied Science, 71(55): 1-42.

Hase, S. B., & Belkar, S. B. (2015). A study of development and performance characteristics of NAO brake linings with Fly Ash. International Journal of Multidisciplinary Research and Development, 2(2): 225-226.

Hsia, K. H., & Wu, J. H. (1998). A study on the data preprocessing in Grey Relation Analysis. Journal of the Chinese Grey System Association Journal of the Chinese Grey System Association, 1(1): 47-53.

Idris, U. D., Aigbodion, V. S., Abubakar, I. J., & Nwoye, C. I. (2015). Eco-friendly asbestos free brake pad; using banana peels. Journal of King Sand University-Engineering Services, 27(1), 185 – 192.

Ikpambese, K. K, Gundu, D. T., & Tuleun, L. T. (2014). Evalution of Palm Kernel Fibres (PKF) for Production of Asbestos – Free Automotive Brake Pads. Journal of King Sand University – Engineering Sciences, 120(7): 1-9.

Ilie, F., & Cristescu, A. C. (2023). Experimental Study of the Correlation between the Wear and the Braking System Efficiency of a Vehicle. Applied Sciences, 13(14): 8139.

Irawan, A. P., Fitriyana, D. F., Tezara, C., Siregar, J. P., Laksmidewi, D., Baskara, G. D., Abdullah, M. Z., Junid, R., Hadi, A. E., Hamdan, M. H. M., & Najid, N. (2022). Overview of the important factors influencing the performance of eco-friendly brake pads. Polymers, 14(6): 1-14.

Joshi, A. G., Bharath, K. N., & Basavarajappa, S. (2023). Recent progress in the research on natural composite brake pads: A comprehensive review. Tribology - Materials, Surfaces & Interfaces, 17(3), 1-15.

Kanagaraj, M., Babu, S., Mohan, S. R. J., & Christy, T. V. (2023). The evaluation of friction and wear performances of commercial automotive brake friction polymer composites Available to Purchase. Industrial Lubrication and Tribology, 75(3), 299–304.

Maleque, M. A., Atiqah, A., Talib, R. J., & Zahurin, H. (2012). New natural fibre reinforced aluminum composite for automotive brake pad. International Journal of Mechanical and Materials Engineering (IJMME), 7(2): 166 – 170.

Naidu, M., Bhosale, A., Gaikwad, M., Salunkhe, S., Čep, R. & Abouel Nasr, E. (2024). Tribological investigations of hemp reinforced NAO brake friction polymer composites with varying percentage of resin loading. Frontiers Materials, 11(8), 1-18.

Naidu, M., Bhosale, A., Gaikwad, M., Salunkhe, S., Cep, R., & Nasr, E. A. (2024). Tribological investigations of hemp reinforced NAO brake friction polymer composites with varying percentage of resin loading. Polymeric and Composite Materials, 11, 1-15.

Naidu, M., Bhosale, A., Munde, Y., Salunkhe, S., & Hussein, H. M. A. (2022). Wear and friction analysis of brake pad material using natural hemp fibers. Polymers, 15(1):1-11.

Pujari, S., Ramakrishna, A., & Kumar, M. S. (2014). Comparison of jute and banana fibre composites: a review.

International Journal of Current Engineering and Technology, (2): 121 – 129.

Ruzaidi, C. M., Kamarudin, H., Shamsul, J. B., & Abdullahi, M. M. A. (2011). Comparative study on thermal, compressive and wear properties of palm slag brake pad composite with other fillers, advanced materials research. Australian Journal of Basic and Applied Sciences, 5(10): 790-796

Sellami, A., & Elleuch, R. (2024). Green composite friction materials: A review of a new generation of eco-friendly brake materials for sustainability. Environmental Engineering Research, 29(3), 1-20.

Shuaibu, Y. A., Ameh, S. E., Abubakar, J. A., Musa, A. J., & Abubakar, G. M. (2023). Development of asbestos-free brake pad using coconut shell powder and coconut shell ash as filler materials with gum arabic as the binder. International Journal of Innovations In Engineering Research and Technology, 10(4): 112-120.

Sunday, G., Borisade, O., Olatunde, A., & James, A. (2021). Evaluation of walnut shell abrasive sandpaper. FUDMA Journal of Sciences (FJS), 5(1), 339-345.

Umamaheswara, R. R., & Babji, G. (2015). A review paper on alternate materials for asbestos brake pads and its characteristics. International Research Journal of Engineering and Technology (IRJET), 2(2): 556-562.

Xiao, X. C., Wang, X. Q., Fu, K. Y., & Zhao, Y. J. (2004). Grey Relational Analysis on factors of the quality of web service. Physics Procedia, 33(1): 1992-1998.

Yawas, D. S., Aku, S. Y., & Amaren, S. G. (2016). Morphology and properties of periwinkle shell asbestos free brake pad. Journal of King Saud University-Engineering Sciences, 28(8), 103 – 109.

Yuvaraj, L., & Jeyanthi, S. (2015). An investigation on chemical treatment of phenol formaldehyde with natural fibres for brake pads. Journal of Chemical and Pharmaceutical Science, 7(1): 419-421.

Zheng, K., Min, Z., Zhang, F., Ren, Z., & Lin, Y. (2025). High heat-fade resistance, metal-free resin-based brake pads: a step towards replacing copper by using andalusite. Chinese Journal of Mechanical Engineering, 38(153): 1-17.

Zhenzhen, F.,Baoting, S.,Rongping, Y., Yimei, L, Hui, W., Shicheng, Q., Shengling, J., Yafei, L., & Vlastimil, M. (2012). Development of eco – friendly brake friction composites containing flax fibers. Journals of Reinforced Plastics & Composites, 31(10), 681-689.



©2025 This is an Open Access article distributed under the terms of the Creative Commons Attribution 4.0 International license viewed via https://creativecommons.org/licenses/by/4.0/ which permits unrestricted use, distribution, and reproduction in any medium, provided the original work is cited appropriately.